# A new nonlinear mean-field model of strange hadronic matter*

K. Miyazaki

**Abstract**

The derivative scalar-coupling (DSC) model of relativistic nuclear matter by Zimanyi and Moszkowski is reconsidered from a constituent quark picture of nucleons. The DSC can be regarded as a correction to $NN\sigma$ coupling owing to the effect of scalar mean-field on the constituent quark. By a little revision of the DSC model, we find a new model that can reproduce the nuclear matter saturation properties as well as the Dirac-Brueckner-Hartree-Fock model. This model is readily extended to hyperons and then is applied to investigate the strange hadronic matter. It predicts the same metastable state as the nonlinear Walecka model or the modified quark-meson coupling model.

## 1 Introduction

The relativistic nuclear model based on the Dirac equation for a nucleon has now became a standard approach to describe nuclear systems. A lot of variations and extensions to the original Walecka model [1] have been developed. Among them, the following four models are especially important. The nonlinear Walecka (NLW) model including phenomenological $\sigma$ and $\omega$ self-coupling terms [2] is most widely used. The Dirac-Brueckner-Hartree-Fock (DBHF) theory [3] has no fitting parameters to nuclear properties and so is the most confidential model at present. The quark-meson coupling (QMC) model [4] is also noticeable. It is a first attempt to take into account the nucleon structure in the nuclear mean-field.

Another interesting phenomenological model is the derivative scalar-coupling (DSC) model [5] developed by Zimanyi and Moszkowski. It predicted the same saturation properties of nuclear matter as the QMC model. Both the models have effectively density-dependent $NN\sigma$ coupling constant. These suggest that the DSC model has its theoretical foundation on the nucleon structure. In fact it has been shown [6] that the relativistic SU(6) model of a nucleon gives the similar $NN\sigma$ coupling to the DSC. Furthermore, it has been shown recently [7] that the generalized version of the DSC model [5], which includes effectively density-dependent $NN\omega$ coupling also, can be derived by the renormalization of wave function in the Walecka model. It is noted that this renormalization takes into

*This paper is the revised version of CDS ext-2003-062. I have improved the results of Figs. 6-8 and corrected some texts and mistypes, but the essential features are not altered.

account the nucleon structure in terms of the meson cloud in nuclear medium. The predicted nuclear matter saturation properties are comparable to the DBHF calculation.

The effectively density-dependent $NN\sigma$ and $NN\omega$ couplings in the DSC model or its variation inspire us to apply and test the model to describe high-density hadronic matter. In this respect, the strange hadronic matter (SHM), especially the metastable exotic multi-hyper-nuclear object (MEMO), is a recent interest. The first investigation has been done using the NLW model [8]. The metastable state with large strangeness fraction $f_s \approx 1.3$ is predicted. The NLW model is able to reproduce the properties of nuclear matter at saturation or finite nuclei. However this never means that it precisely predicts the properties of the hadronic matter at high density, since there are no density-dependences in it. Then the study using the modified QMC model [9], which has effectively density-dependent $NN\sigma$ coupling, has been performed. Contrary to our expectation, both the models predict the similar results since their metastable states with large strangeness fraction are mainly due to the additional strong attraction in YY channels.

On the other hand, the DSC model has ever been applied only to $N + \Lambda$ matter [10] because the theoretical principle for extending the DSC to hyperons does not exist. To overcome the problem, in the present work, we reconsider the DSC model from the constituent quark picture of baryons and improve it to reproduce the nuclear matter saturation properties as well as the DBHF theory. Since this new model can be easily extended to hyperons, we apply it to describe the SHM. The detailed formulation is presented in the next section and the calculational results are discussed in section 3. We have however not taken into account the strange mean-fields included in Ref. [8] and [9] because the coupling constants of strange mesons cannot be determined unambiguously at present and because the main purpose of the present work is to show the essential framework of our new nonlinear mean-field model of hadron matter. Conclusions of this work are drawn in section 4.

# 2 Revision of the DSC model and its extension to hyperons

In the present work, we treat charge symmetric hadronic matter and so take only into account the isoscalar $\sigma$ and $\omega$ mesons and their mean fields. In the constituent quark model of a nucleon, the $NN\sigma$ or $NN\omega$ coupling used in the Walecka model is depicted by

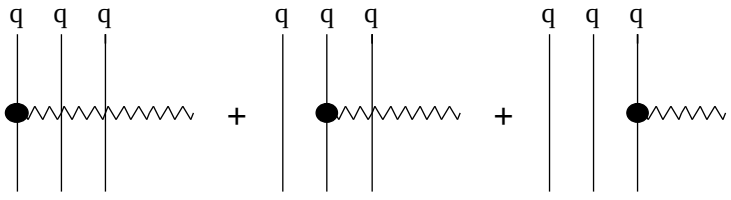

or expressed by

$$g_{NN\sigma(\omega)} = 3\, g_{qq\sigma(\omega)}. \tag{1}$$

Only one quark $q = u$ or $d$ in a nucleon couples to the mesons (wavy lines) while the other two quarks are the spectators. However, for a nuclear nucleon, all the three quarks are embedded in nuclear mean field. This effect should be taken into account so as to go beyond the Walecka model. It was also a subject of the QMC model [4], in which the mean field fulfills a nucleon bag.

Here we consider the following first-order correction by the scalar potential of a quark:

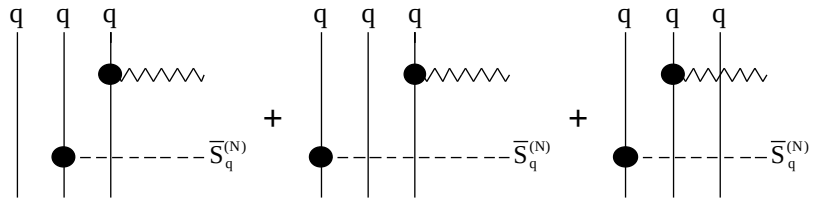


where $\bar{S}_q^{(N)} \equiv S_q^{(N)}/M_q$. Using the scalar potential $S_N$ and the mass $M_N$ of a nucleon, those of a quark are $S_q^{(N)} = (1/3)\, S_N$ and $M_q = (1/3)\, M_N$. As a result we have the effective $NN\sigma$ coupling constant

$$g_{NN\sigma} \rightarrow\ g^*_{NN\sigma} = g_{NN\sigma} + 3\, g_{qq\sigma}\, \bar{S}_q^{(N)} = m^*_N\, g_{NN\sigma}, \tag{2}$$

where $m^*_N \equiv M^*_N/M_N$ with $M^*_N = M_N + S_N$. It is noted that Eq. (2) is just the DSC itself. Similarly, we have the effective $NN\omega$ coupling constant

$$g_{NN\omega} \rightarrow\ g^*_{NN\omega} = g_{NN\omega} + 3\, g_{qq\omega}\, \bar{S}_q^{(N)} = m^*_N\, g_{NN\omega}. \tag{3}$$

Both of Eqs. (2) and (3) corresponds to the generalized DSC model of Eq. (A-3) in Ref. [5] using $\alpha_s = \alpha_v = 2$.

We have reconsidered the DSC model from the constituent quark picture of a nucleon. However the DSC model cannot reproduce the saturation properties of nuclear matter. Especially, it gives larger effective mass of a nuclear nucleon $m^*_N \simeq 0.85$ than the appropriate value $m^*_N \simeq 0.6$ to yield strong spin-orbit potential. On the other hand, it was found in Ref. [7] that nuclear saturation properties are well reproduced using the effective $NN\sigma$ and $NN\omega$ coupling constants

$$g^*_{NN\sigma(\omega)} = \left[\left(1 - \lambda_N^{\sigma(\omega)}\right) + \lambda_N^{\sigma(\omega)} m^*_N\right] g_{NN\sigma(\omega)}. \tag{4}$$

We have obtained $\lambda_N^\sigma = \lambda_N^\omega = 0.35$, which is close to $1/3$ and thus suggests that Eq. (4) has its origin in the constituent quark picture of a nucleon. In fact, if $\lambda_N^\sigma = \lambda_N^\omega = 1/3$, Eq. (4) can be derived by using $\bar{S}_q^{(N)} \equiv S_q^{(N)}/M_N$ in Eqs. (2) and (3) in place of $\bar{S}_q^{(N)} \equiv S_q^{(N)}/M_q$. We adapt this prescription in the following.

According to the quark picture, the extension of Eq. (4) to hyperons is straightforward. For $\Lambda$ and $\Sigma$ hyperons, the usual $YY\sigma$ or $YY\omega$ coupling is depicted by

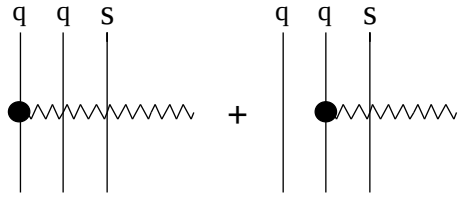


or expressed by

$$g_{\Lambda\Lambda\sigma(\omega)} = g_{\Sigma\Sigma\sigma(\omega)} = 2\, g_{qq\sigma(\omega)} = (2/3)\, g_{NN\sigma(\omega)}. \tag{5}$$

They are corrected by the following contribution,

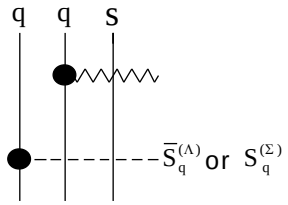


where $\bar{S}_q^{(\Lambda)} \equiv S_q^{(\Lambda)}/M_\Lambda$ or $\bar{S}_q^{(\Sigma)} \equiv S_q^{(\Sigma)}/M_\Sigma$ is the effect by the scalar potential of a quark in $\Lambda$ or $\Sigma$. Because the scalar potentials of $\Lambda$ and $\Sigma$ are $S_\Lambda = 2\, S_q^{(\Lambda)}$ and $S_\Sigma = 2\, S_q^{(\Sigma)}$, the effective $\Lambda\Lambda\sigma(\omega)$ and $\Sigma\Sigma\sigma(\omega)$ coupling constants are given by

$$g^*_{\Lambda\Lambda\sigma(\omega)} = g_{\Lambda\Lambda\sigma(\omega)} + \bar{S}_q^{(\Lambda)} g_{qq\sigma(\omega)} = \left(1 + \frac{1}{4}\,\bar{S}_\Lambda\right)\, g_{\Lambda\Lambda\sigma(\omega)}, \tag{6}$$

$$g^*_{\Sigma\Sigma\sigma(\omega)} = g_{\Sigma\Sigma\sigma(\omega)} + \bar{S}_q^{(\Sigma)} g_{qq\sigma(\omega)} = \left(1 + \frac{1}{4}\,\bar{S}_\Sigma\right)\, g_{\Sigma\Sigma\sigma(\omega)}, \tag{7}$$

where $\bar{S}_{\Lambda(\Sigma)} \equiv S_{\Lambda(\Sigma)}/M_{\Lambda(\Sigma)}$. On the other hand, $\Xi$ hyperons contain only one $u$ or $d$ quark and so $\Xi\Xi\sigma(\omega)$ coupling constant is not corrected by nuclear (scalar) mean field:

$$g^*_{\Xi\Xi\sigma(\omega)} = g_{\Xi\Xi\sigma(\omega)}. \tag{8}$$

If the strange mean-fields are considered [8,9], $\Xi\Xi\sigma(\omega)$ coupling will be also corrected. The present work however does not study such a correction.

We can summarize the above results as

$$g^*_{BB\sigma(\omega)} = \left[\left(1 - \lambda_B^{\sigma(\omega)}\right) + \lambda_B^{\sigma(\omega)} m_B^*\right] g_{BB\sigma(\omega)}, \tag{9}$$

where

$$\lambda_N^\sigma = \lambda_N^\omega = 1/3, \tag{10}$$

$$\lambda_\Lambda^\sigma = \lambda_\Lambda^\omega = 1/4, \tag{11}$$

$$\lambda_\Sigma^\sigma = \lambda_\Sigma^\omega = 1/4, \tag{12}$$

$$\lambda_\Xi^\sigma = \lambda_\Xi^\omega = 0, \tag{13}$$

and $m_B^* \equiv M_B^*/M_B$ with $M_B^* = M_B + S_B$. The strangeness of each baryon is revealed in the different values of $\lambda_B^{\sigma(\omega)}$.

We want to emphasize that our model has advantages over the NLW and the QMC models. Our model has no more parameters than the Walecka model and effectively density-dependent $BB\sigma(\omega)$ coupling constants while the NLW model has three additional parameters but has no density dependences. Both our and the QMC models take into account the effect of nuclear mean-fields on quarks in a baryon. However it is incompatible with the confinement mechanism realized by the bag model used in the QMC model. Our model is not worried by such a problem because it is based on the naïve constituent quark model.

Next we apply the model (9) to the SHM in bulk. Our model Lagrangian is

$$\mathcal{L} = \sum_{B=N,\Lambda,\Sigma,\Xi} \bar{\psi}_B \left( \not{p} - M_B^* - \gamma^0 V_B \right) \psi_B - \frac{1}{2} m_\sigma^2 \langle \sigma \rangle^2 + \frac{1}{2} m_\omega^2 \langle \omega_0 \rangle^2, \tag{14}$$

and so the energy density is

$$\mathcal{E} = \sum_{B=N,\Lambda,\Sigma,\Xi} \left( \langle E_k^* \rangle_B + V_B \right) \rho_B + \frac{1}{2} m_\sigma^2 \langle \sigma \rangle^2 - \frac{1}{2} m_\omega^2 \langle \omega_0 \rangle^2, \tag{15}$$

where $\langle E_k^* \rangle_B$ is the average kinetic energy and $\rho_B$ is the density of each baryon. The vector potential $V_B$ is given by

$$V_B = g_{BB\omega}^* \langle \omega_0 \rangle = \left[ (1 - \lambda_B^\omega) + \lambda_B^\omega m_B^* \right] g_{BB\omega} \langle \omega_0 \rangle . \tag{16}$$

Inverting Eq. (16) as

$$\langle \omega_0 \rangle = \frac{V_N}{g_{NN\omega}^*} = \frac{V_Y}{g_{YY\omega}^*}, \tag{17}$$

we have

$$V_Y = \frac{g_{YY\omega}^*}{g_{NN\omega}^*} V_N. \tag{18}$$

On the other hand, the scalar potential $S_B$ is given by

$$S_B = -g_{BB\sigma}^* \langle \sigma \rangle = -\left[ (1 - \lambda_B^\sigma) + \lambda_B^\sigma m_B^* \right] g_{BB\sigma} \langle \sigma \rangle . \tag{19}$$

Inverting Eq. (19) as

$$\langle\sigma\rangle = \frac{(1-m_N^*)\,M_N}{g_{NN\sigma}^*} = \frac{(1-m_Y^*)\,M_Y}{g_{YY\sigma}^*}, \tag{20}$$

we have

$$1-m_Y^* = \frac{M_N}{M_Y}\,\frac{g_{YY\sigma}}{g_{NN\sigma}}\,\frac{(1-\lambda_Y^\sigma)+\lambda_Y^\sigma\,m_Y^*}{(1-\lambda_N^\sigma)+\lambda_N^\sigma\,m_N^*}\,(1-m_N^*)\,, \tag{21}$$

$$= \left[\lambda_Y^\sigma + \frac{M_Y}{M_N}\,\frac{g_{NN\sigma}}{g_{YY\sigma}}\,\frac{(1-\lambda_N^\sigma)+\lambda_N^\sigma\,m_N^*}{1-m_N^*}\right]^{-1}. \tag{22}$$

Substituting Eqs. (17) and (20), Eq. (15) becomes

$$\mathcal{E} = \sum_{B=N,\Lambda,\Sigma,\Xi}\langle E_k^*\rangle_B\,\rho_B + \left(\sum_{B=N,\Lambda,\Sigma,\Xi}\frac{g_{BB\omega}^*}{g_{NN\omega}^*}\,\rho_B\right)V_N + \frac{1}{2}\,m_\sigma^2\,\langle\sigma\rangle^2 - \frac{1}{2}\left(\frac{m_\omega}{g_{NN\omega}^*}\right)^2 V_N^2. \tag{23}$$

The vector potential $V_N$ for a nucleon is determined by $\partial\mathcal{E}/\partial V_N = 0$:

$$V_N = \frac{g_{NN\omega}^*}{m_\omega}\sum_{B=N,\Lambda,\Sigma,\Xi}\frac{g_{BB\omega}^*}{m_\omega}\,\rho_B. \tag{24}$$

Substituting Eq. (24) into Eq. (23) again, the energy density becomes

$$\mathcal{E} = \sum_{B=N,\Lambda,\Sigma,\Xi}\langle E_k^*\rangle_B\rho_B + \frac{1}{2}\left(\frac{M_N\,m_\sigma}{g_{NN\sigma}^*}\right)^2(1-m_N^*)^2 + \frac{1}{2}\left(\sum_{B=N,\Lambda,\Sigma,\Xi}\frac{g_{BB\omega}^*}{m_\omega}\,\rho_B\right)^2. \tag{25}$$

Finally we can determine $m_N^*$ from the self-consistency equation,

$$\frac{d}{d\,m_N^*}\left(\frac{\mathcal{E}}{M_N\rho_T}\right) = \sum_{B=N,\Lambda,\Sigma,\Xi} f_B\frac{M_B}{M_N}\,\frac{\rho_B^{(s)}}{\rho_B}\,\frac{d\,m_B^*}{d\,m_N^*} - \frac{M_N}{\rho_T}\left(\frac{m_\sigma}{g_{NN\sigma}}\right)^2\frac{1-m_N^*}{[(1-\lambda_N^\sigma)+\lambda_N^\sigma\,m_N^*]^3}$$
$$+\,\frac{\rho_T}{M_N}\left(\sum_{B=N,\Lambda,\Sigma,\Xi} f_B\,\frac{g_{BB\omega}^*}{m_\omega}\right)\left(\sum_{B=N,\Lambda,\Sigma,\Xi} f_B\,\lambda_B^\omega\,\frac{g_{BB\omega}}{m_\omega}\,\frac{d\,m_B^*}{d\,m_N^*}\right) = 0, \tag{26}$$

where $\rho_T = \sum_{B=N,\Lambda,\Sigma,\Xi}\rho_B$ is the total baryon density, $f_B = \rho_B/\rho_T$ is the baryon fraction, $\rho_B^{(s)}$ is the scalar density and

$$\frac{d\,m_Y^*}{d\,m_N^*} = \frac{M_Y}{M_M}\,\frac{g_{NN\sigma}}{g_{YY\sigma}}\left(\frac{1-m_Y^*}{1-m_N^*}\right)^2. \tag{27}$$

Once solving Eq. (26) and having the value of $m_N^*$, we can calculate $m_Y^*$ from Eq. (22) and then the energy density from Eq. (25).

# 3 Numerical analyses

We first calculate the usual nuclear matter and determine the coupling constants $g_{NN\sigma}$ and $g_{NN\omega}$ to reproduce the saturation condition $E/\rho_N - M_N = -15.75\,\mathrm{MeV}$ at $\rho_N = 0.16\,\mathrm{fm}^{-3}$. The detailed procedure of the calculation is essentially the same as Ref. [7]. Only the difference is that the parameter $\lambda$ of Eq. (105) in Ref. [7] is given by Eq. (10). In the following table, we summarize the values of the coupling constants, the effective mass $m_N^*$, the scalar $S_N$ and vector $V_N$ potentials, the incompressibility $K_v$ and the Coulomb coefficient $K_{Coul}$ [11]:

| $g_{NN\sigma}$ | $g_{NN\omega}$ | $m_N^*$ | $S$ (MeV) | $V$ (MeV) | $K_v$ (MeV) | $K_{Coul}$ (MeV) |
|---|---|---|---|---|---|---|
| 11.4 | 14.0 | 0.605 | $-371$ | 297 | 302 | $-5.55$ |

The results are comparable to the DBHF calculation [3]. Therefore our new nonlinear mean-field model of nuclear matter is reasonable and useful to investigate dense baryonic matter.

Next we investigate the charge symmetric $N+\Lambda$ matter and compare our model with the DSC model in Ref. [10], which corresponds to using $\lambda_N^\sigma = \lambda_\Lambda^\sigma = 1$ and $\lambda_N^\omega = \lambda_\Lambda^\omega = 0$ in place of Eqs. (10) and (11). According to the usually used prescription [5,8], the $\Lambda\Lambda\omega$ coupling constant is determined by the constituent quark model (5) while the $\Lambda\Lambda\sigma$ coupling constant is chosen to yield reasonable $\Lambda$ potential $U_\Lambda^{(N)}(\rho_{NM}) = -30\,\mathrm{MeV}$ in saturated nuclear matter. Figure 1 calculates the lowest binding energy per baryon,

$$E/B = \mathcal{E}/\rho_T - f_N M_N - f_\Lambda M_\Lambda, \tag{28}$$

for each value of the total baryon density $\rho_T = \rho_N + \rho_\Lambda$, and the corresponding lambda fraction $f_\Lambda$. The solid and dotted curves are the results by our and the DSC models, respectively. We note that the minimum of $E/B$ is only slightly shifted from the saturation point of nuclear matter, namely, $E/B = -16.3\,\mathrm{MeV}$ and $E/B = -16.5\,\mathrm{MeV}$ at $\rho_T = 0.18\,\mathrm{fm}^{-3}$ for our and the DSC model. The corresponding lambda fraction is $f_\Lambda = 0.10$ and $f_\Lambda = 0.12$ respectively. This metastable state with small lambda fraction is more clearly seen in Fig. 2, which shows the lowest $E/B$ for each value of lambda fraction. The similar results were also obtained in the QMC model [9].

The difference of $E/B$ between the solid and dotted curves in Fig. 1(a) is small below the minimum point, while it becomes larger at higher densities due to the larger incompressibility of our model than the DSC model. The lambda fractions in Fig. 1(b) become larger as the density increases except for low densities. For our model, this is also seen in Fig. 3, which shows $E/B$ as the functions of total baryon density for the fixed values of lambda fraction. At densities larger than $\rho_T = 0.18\,\mathrm{fm}^{-3}$, $E/B$ for $f_\Lambda = 0.2$ becomes lower than $E/B$ for $f_\Lambda = 0.0$. At densities larger than $\rho_T = 0.36\,\mathrm{fm}^{-3}$, $E/B$ for $f_\Lambda = 0.4$ becomes lowest. There is a negative-energy minimum only below $f_\Lambda = 0.64$ for

our model and below $f_\Lambda = 0.72$ for the DSC model. The corresponding density to the minimum increases up to $f_\Lambda = 0.4$ and then turns to decrease. This is explicitly seen in Fig. 4 that shows the density corresponding to the binding energies in Fig. 2.

Figure 5 shows $m_N^*$ and $m_\Lambda^*$ corresponding to the binding energies in Fig. 2. We first note the large differences between the two models. However the dependences on the lambda fraction are weak especially below $f_\Lambda = 0.4$ in both the models. We further note that both the effective masses in the two models have minimum values at $f_\Lambda = 0.33$, which is rather different from the minimum point $f_\Lambda \approx 0.1$ in Fig. 2. These facts indicate that the relativistic dynamics by the nuclear mean-fields are not directly reflected in the metastable state of $N + \Lambda$ matter. This is the reason that both our and the DSC models have predicted the similar properties of the metastable state.

Next we investigate the SHM consisting of $N$+$\Lambda$+$\Sigma$+$\Xi$ under the chemical equilibrium [8]. The $YY\omega$ coupling constants are determined by the constituent quark model (5) while the $YY\sigma$ coupling constants are chosen to yield reasonable $\Sigma$ and $\Xi$ potentials in saturated nuclear matter, namely, $U_\Sigma^{(N)}(\rho_{NM}) = 30\,\mathrm{MeV}$ and $U_\Xi^{(N)}(\rho_{NM}) = -28\,\mathrm{MeV}$. We first calculate in Fig. 6 the binding energy per baryon

$$\frac{E}{B} = \frac{\mathcal{E}}{\rho_T} - \sum_{B=N,\Lambda,\Sigma,\Xi} f_B\, M_B, \tag{29}$$

as functions of the total baryon density $\rho_T = \sum_{B=N,\Lambda,\Sigma,\Xi} \rho_B$ for fixed strangeness fractions

$$f_S = f_\Lambda + f_\Sigma + 2\, f_\Xi. \tag{30}$$

The energy minimum of the SHM with $f_S = 0.4$ or 0.8 is lower than the saturation energy of nuclear matter while that with $f_S = 1.2$ or 1.6 is larger. The total baryon density corresponding to the minimum grows with the strangeness fraction.

So as to investigate the results of Fig. 6 in detail, Figs. 7(a) and (b) show the lowest $E/B$ for each value of $f_S$ and the corresponding total baryon density. Furthermore Figs. 8(a) and (b) show the corresponding density fraction $f_B$ and the effective mass $m_B^*$ of each baryon. The $\Sigma$ hyperons do not appear because of the repulsive optical potential assumed above. The dip at $f_S = 0.1$ in Fig. 7(a) corresponds to the minimum of the solid curve in Fig. 2. For the convenience of comparison, we re-present the result of $N + \Lambda$ matter by the dotted curve. The advent of $\Xi$ hyperons at $f_S = 0.175$ predicts lower binding energy than $N + \Lambda$ matter and the metastable state of $E/B \simeq -17.1\,\mathrm{MeV}$ at $\rho_B \simeq 0.25\,\mathrm{fm}^{-3}$ with $f_S \simeq 0.6$. The negative-energy state is obtained up to $f_S = 1.7$. These are the same as the results by model 1 in Ref. [8]. Inversely speaking, the properties of the metastable state in the SHM do not depend on detailed differences between the models. Especially, the effective density-dependent $BB\sigma$ and $BB\omega$ coupling constants in our model, which are essential differences from the NLW model, have not been distinctly revealed. The reason can be found in Fig. 8(b). The dependences of the effective baryon masses on $f_S$ are not significant. Their lowest values appear at $f_S = 1.575$ that is much larger than

$f_S = 0.6$. As in the case of $N + \Lambda$ matter, these indicate that the relativistic dynamics of our model are not reflected explicitly in the metastable state.

# 4 Conclusions

We have reconsidered the DSC model of relativistic nuclear matter from the constituent quark picture of a nuclear nucleon. The DSC has been interpreted as a correction to $NN\sigma$ coupling in the Walecka model owing to the effect of the scalar mean-field on the constituent quark. A little revision of the DSC model and its application to $NN\omega$ coupling improve significantly the reproduction of nuclear matter saturation properties. We have readily extended this new model to hyperons. Their strangeness appears as the different dependences of $YY\sigma(\omega)$ coupling constants on their effective masses.

We first apply the model to $N+\Lambda$ matter and compare it with the naïve extension of the DSC model to $\Lambda$. Although the relativistic dynamics in both the models are rather different, the properties of predicted metastable state are similar. We further extend our model to the SHM consisting of $N + \Lambda + \Sigma + \Xi$ under the chemical equilibrium and compare it with the NLW model. It is found again that the metastable states in both the models have similar properties. This is because that the metastable state occurs at the density near the saturation point of nuclear matter and has relatively small strangeness fraction, namely, $\rho_T = 0.18\,\mathrm{fm}^{-3}$ with $f_\Lambda = 0.1$ in $N+\Lambda$ matter and $\rho_T \simeq 0.25\,\mathrm{fm}^{-3}$ with $f_S \simeq 0.6$ in the SHM. Since all the models have been adjusted to reproduce the saturation properties of nuclear matter and since the dependences of the effective baryon masses on the strangeness fraction are relatively weak in our model, the detailed differences between the models have not been revealed in the metastable state.

We have not taken into account the strange mean-fields considered in Refs. [8] and [9]. They produce the metastable state in SHM with large strangeness fraction at much higher density than the saturation point. Because of the effectively density-dependent meson-baryon coupling constants, the inclusion of the strange mesons $\sigma^*$ and $\phi$ into our model might predict the different properties of the metastable state from Refs. [8] and [9]. This possibility will be studied in a future work.

# References


[1] B.D. Serot and J.D. Walecka, *Advances in Nuclear Physics*, Vol. **16** (Plenum, New York, 1986).

[2] S. Gmuca, Nucl. Phys. **A547** (1992) 447.

[3] R. Brockmann and R. Machleidt, Phys. Rev. **C42** (1990) 1965.

[4] P.A.M. Guichon, Phys. Lett. **B200** (1988) 235: K. Saito and A.W. Thomas, Phys.Lett. **B327** (1994) 9; Phys. Rev. **C52** (1995) 2789.

[5] J. Zimanyi and S.A. Moszkowski, Phys. Rev. **C42** (1990) 1416. It is noted that the NLW model has linear meson-baryon couplings in spite of its name. On the contrary, the DSC and QMC models are true nonlinear mean-field models.

[6] K. Miyazaki, Prog. Theor. Phys. **91** (1994) 1271.

[7] K. Miyazaki, CERN Document Server (CDS) ext-2002-056 revised by Mathematical Physics Preprint Archive (mp_arc) 05-141.

[8] J. Schaffner-Bielich and A. Gal, Phys. Rev. **C62** (2000) 034311, [arXiv:nucl-th/0005060] and references therein.

[9] P. Wang, R.K. Su, H.Q. Song and L.L. Zhang, Nucl. Phys. **A653** (1999) 106.

[10] M. Barranco, R.J. Lombard, S. Marcos and S.A. Moszkowski, Phys. Rev. **C44** (1991) 178.

[11] J.M. Pearson, Phys. Lett. **B271** (1991) 12.

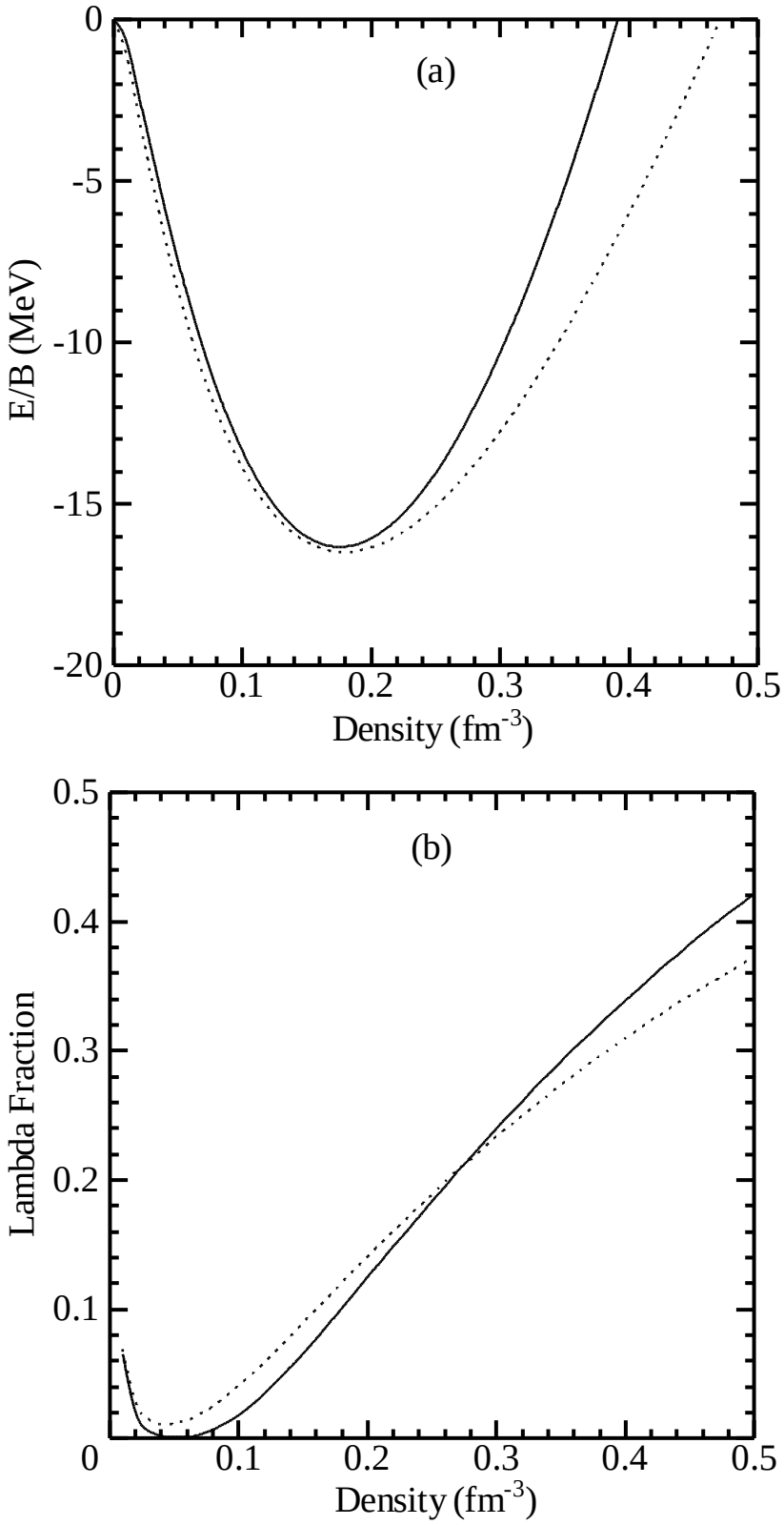


Figure 1: The lowest binding energy per baryon (a) and the corresponding lambda fraction (b) of $N + \Lambda$ matter for each value of the total density. The solid curves are our model calculations using Eqs. (10) and (11) while the dotted curves are the DSC results using $\lambda_N^\sigma = \lambda_\Lambda^\sigma = 1$ and $\lambda_N^\omega = \lambda_\Lambda^\omega = 0$.

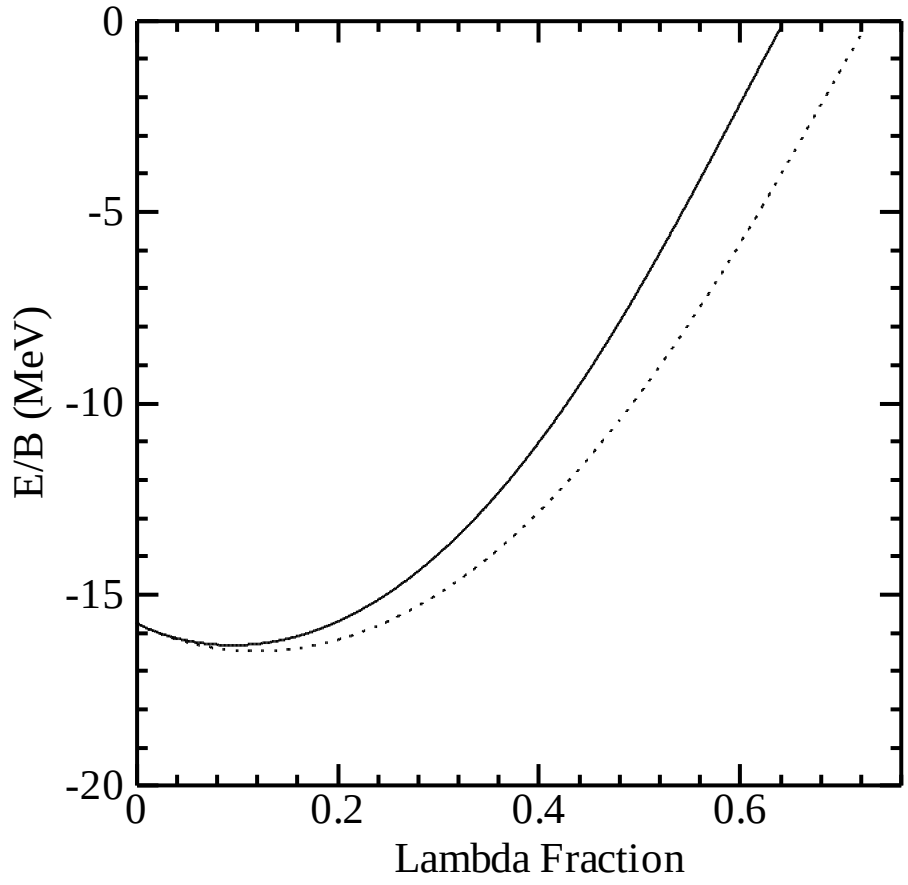


Figure 2: The lowest binding energy per baryon of $N + \Lambda$ matter for each value of the lambda fraction.

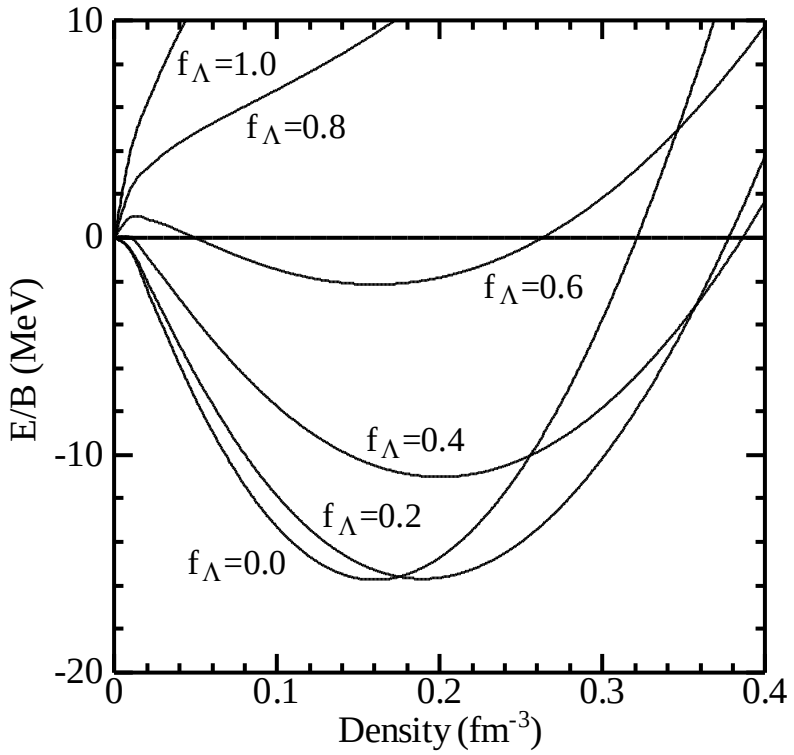


Figure 3: The binding energy per baryon of $N + \Lambda$ matter with fixed lambda fractions as functions of the total baryon density. The curves are the results of our model.

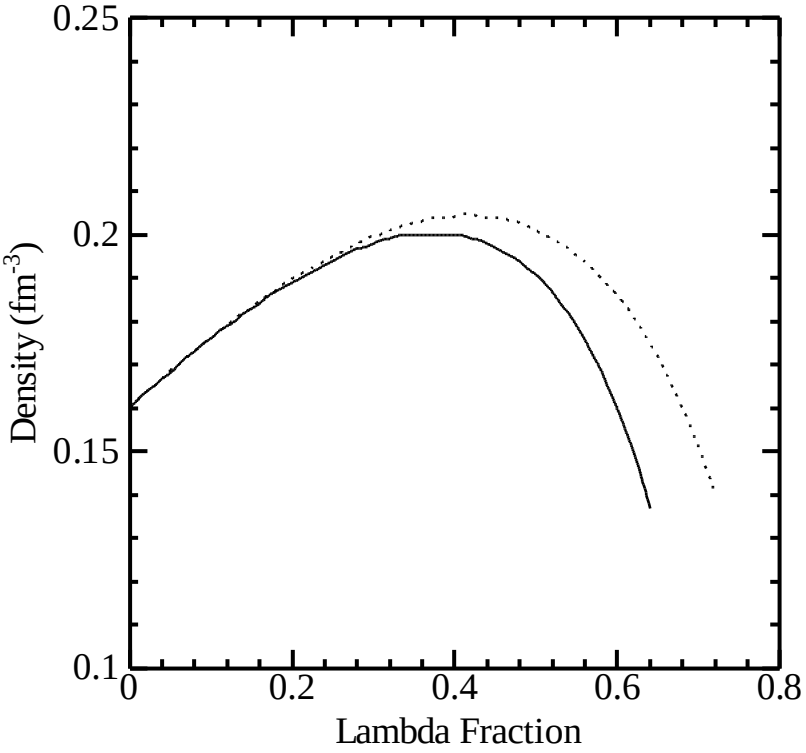


Figure 4: The density of $N + \Lambda$ matter corresponding to the binding energies in Fig. 2.

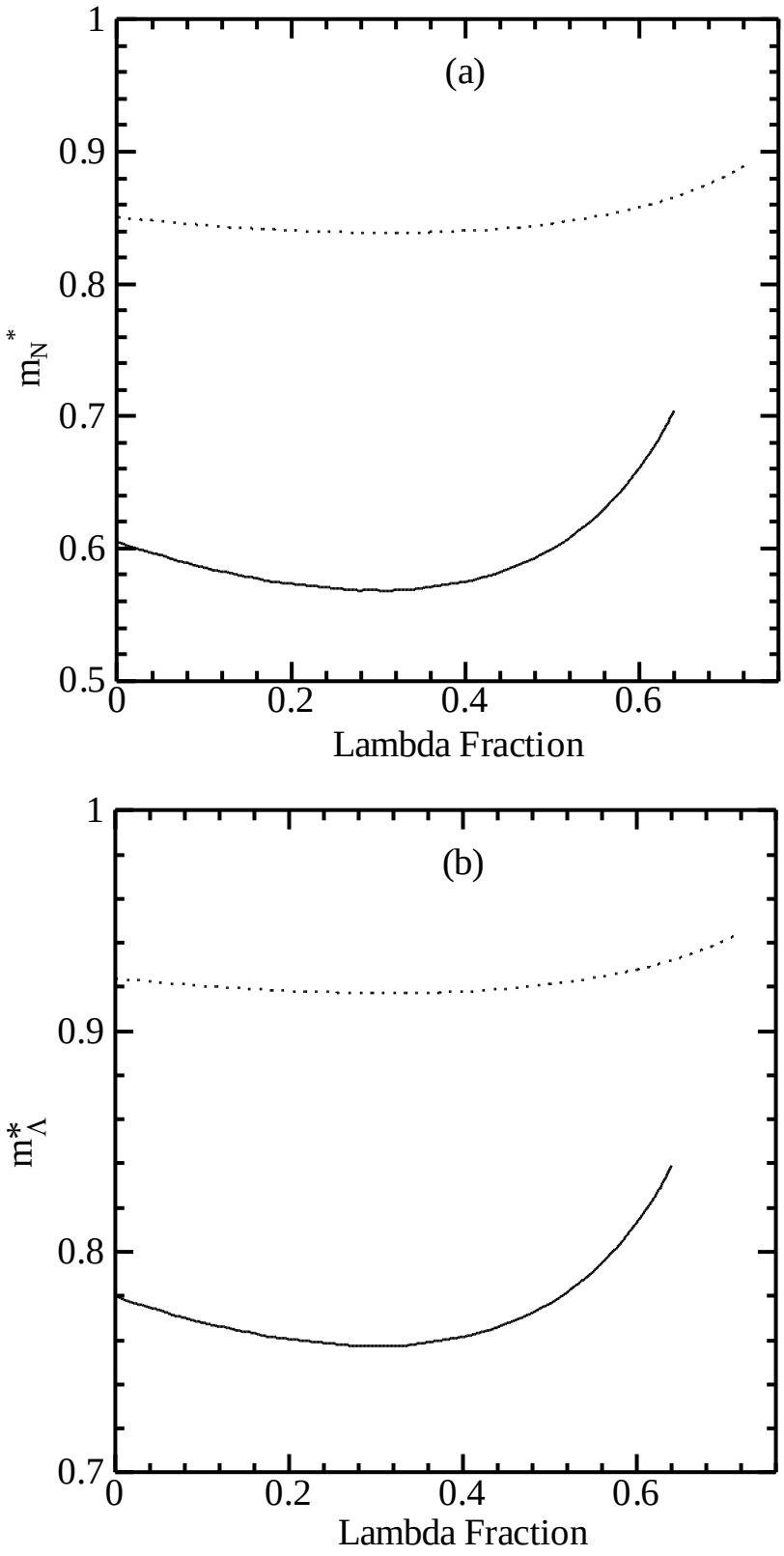


Figure 5: The ratios of the effective masses of a nucleon (a) and lambda (b) to their free masses in $N + \Lambda$ matter corresponding to the binding energies in Fig. 2.

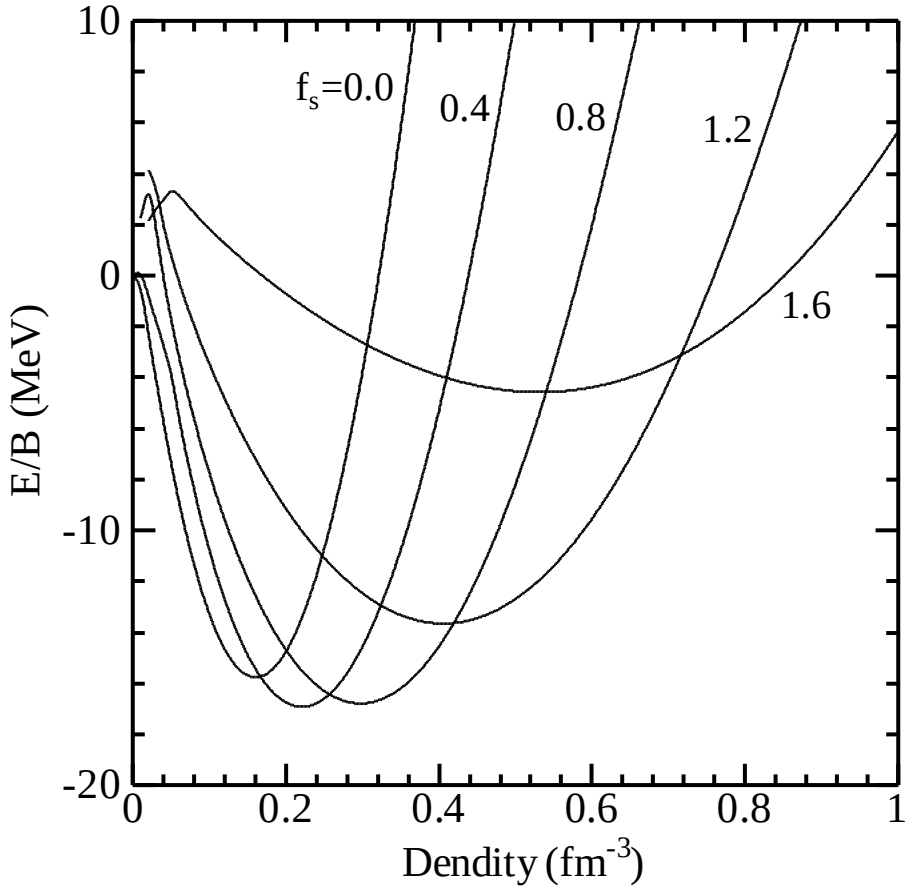


Figure 6: The binding energies per baryon (30) with fixed strangeness fraction as functions of the total baryon density.

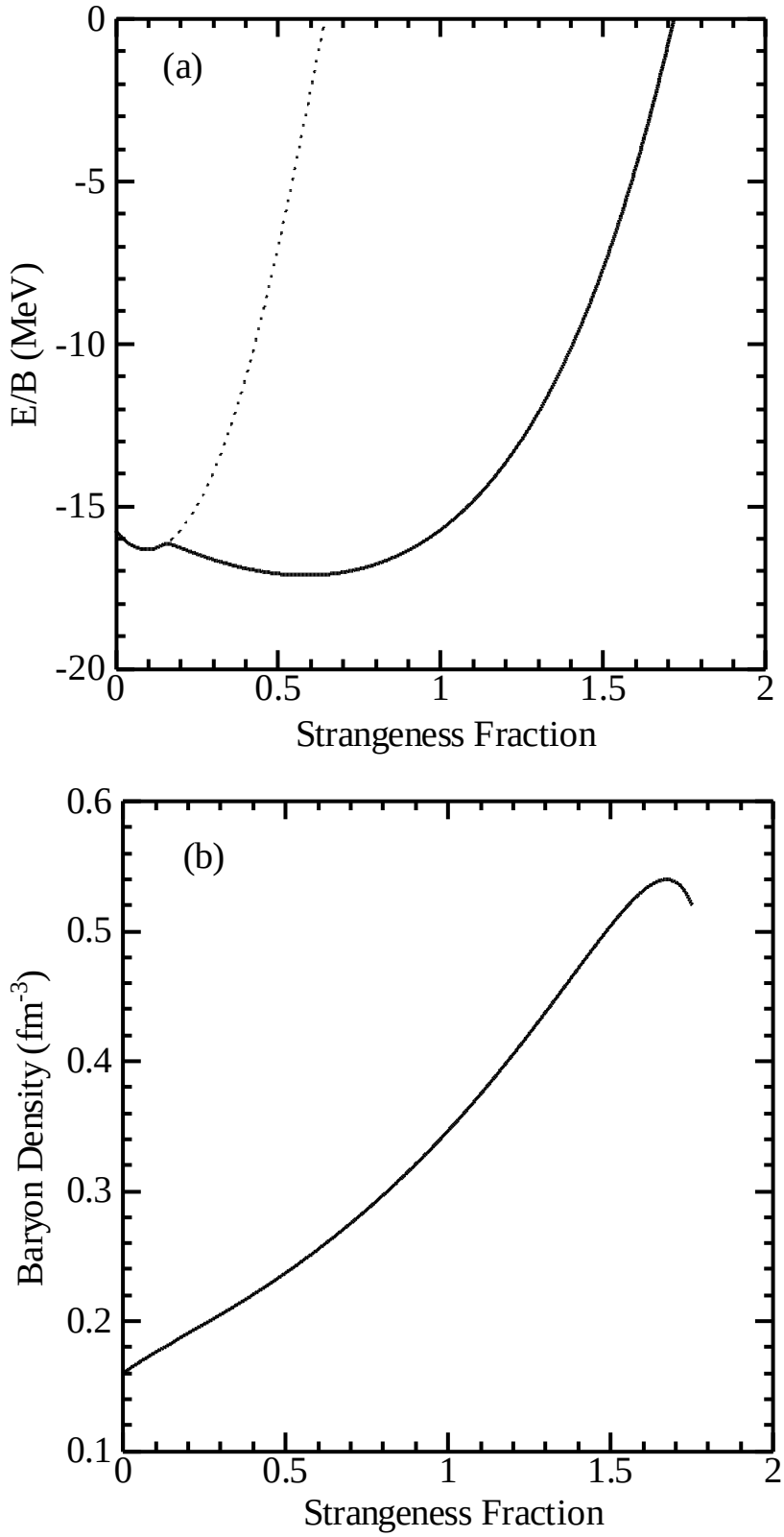


Figure 7: The lowest binding energy per baryon (a) and the corresponding total baryon density (b) of the SHM consisting of $N + \Lambda + \Xi$ for each value of the strangeness fraction. The dotted curve in (a) is the result for $N + \Lambda$ matter.

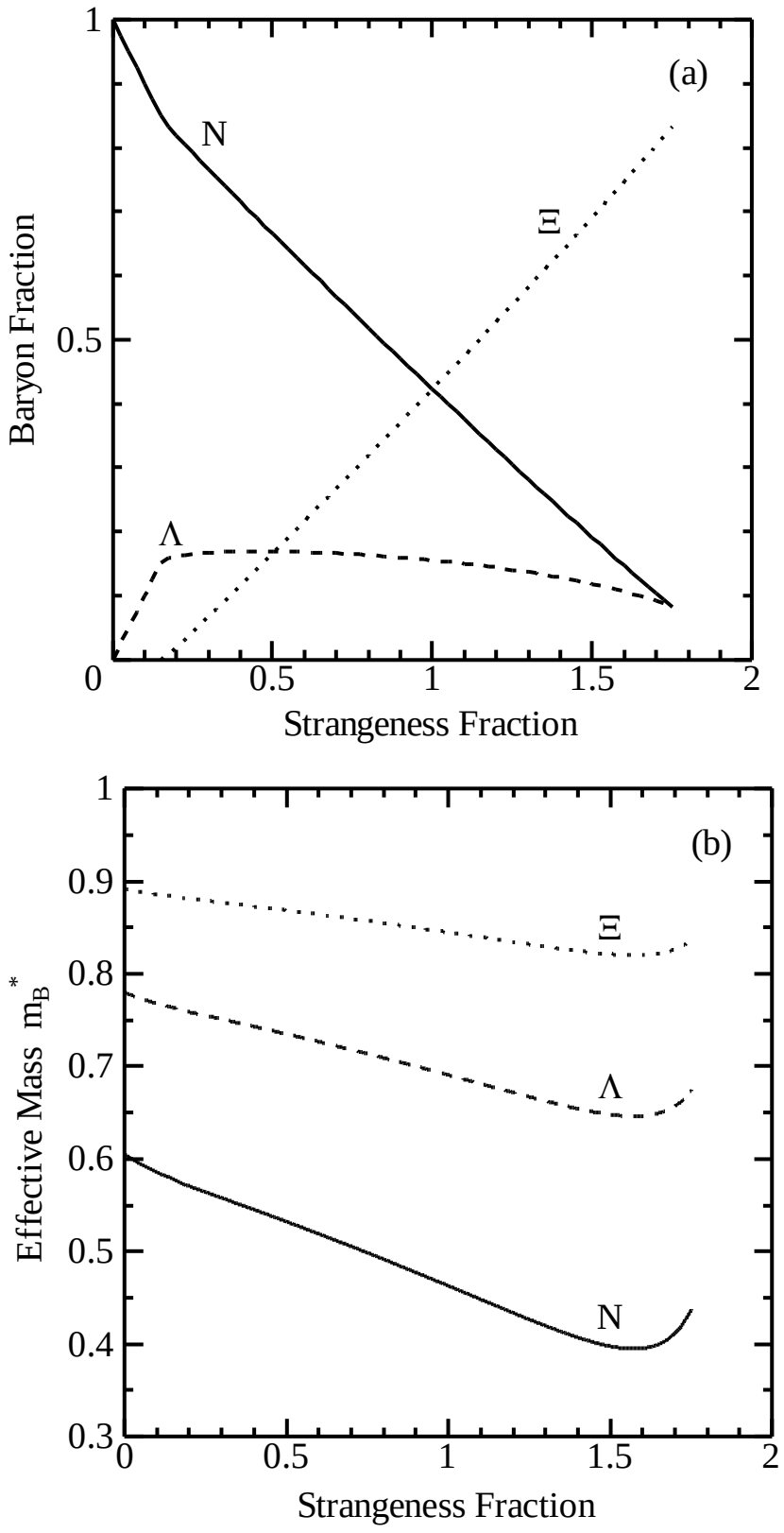


Figure 8: The density fraction (a) and the effective mass (b) for each baryon corresponding to the binding energy (the solid curve) in Fig. 7(a).